Paper

Wire Particle Motion Behavior and Breakdown Characteristics around Different Shaped Spacers within Diverging Air Gap

Yasin Khan* Student Member
Akihito Oda* Student Member
Shigemitsu Okabe** Member
Junya Suehiro* Member
Masanori Hara* Member

Free wire particle motion behavior and particle triggered breakdown characteristics around different shaped spacers between diverging conducting plane electrodes are studied experimentally in the laboratory air under DC and 60 Hz AC voltages. Wire particle motion behavior was observed experimentally and is discussed on the basis of the results of field calculations. Consequently, it was found that a particle around spacer tends to move toward or away from the spacer depending on the field strength around the spacer, under both DC or AC voltages. Moreover, it was observed that a particle can hardly adheres to the spacer in case of corona discharge at wire particle ends under DC voltage and/or an oscillating wire particle in case of AC voltage and viceversa. Also, the wire particle adhesion phenomenon and the characteristics of surface flashover triggered by free conducting wire particle around a simple shaped spacer in quasi uniform field is briefly discussed.

Keywords: GIS, non-uniform electric field, spacer, wire particle motion, particle adhesion, corona discharge

1. Introduction

Gas Insulation System (GIS) is widely used in the electric power systems due to its many advantages such as compactness, non-flammability as well as virtually maintenance free nature. However, there is a limit to the degree of compactness of a GIS because of the accompanying increase in the electric field strength within the GIS equipment. It is well known that free conducting particles in GIS are the most significant factor for the deterioration of insulation integrity [1]. Especially, when this free particle reach an insulating spacer, the insulation condition become more severe.

With the aim to further improve the reliability of GIS equipment, many researchers have investigated particle motion behavior, breakdown characteristics, spacer configurations, etc. [2]~[7], and they have achieved much progress in the insulation technology. However, free conducting wire particle motion behavior around different shaped spacers have not been studied significantly.

In this respect, the authors have been investigating experimentally, the free wire particle motion behavior around different shaped spacers between diverging conducting plane electrodes in the laboratory air under DC and 60 Hz AC voltages. Wire particle motion behavior was observed experimentally and is discussed on the basis of the results of the field calculations. Consequently, it was found that a particle around spacer tends to move toward or away from the spacer depending on the field strength around the spacer, under both DC or AC voltages. Moreover, it was also observed that a free particle can hardly adheres to the spacer in case of corona discharge at wire particle ends under DC voltage and/or an oscillating wire particle in case of AC voltage and viceversa. The phenomenon of particle adhesion to the spacer is also discussed theoretically. Moreover, the surface flashover triggered by free conducting wire particle around a simple shaped spacer in quasi-uniform field is briefly discussed.

2. Experimental Setup and Method

The schematic diagram of the experimental setup is shown in reference [8]. In order to consider the effect of the forces acting on a particle and to simulate the gap configuration commonly found in GIS which has

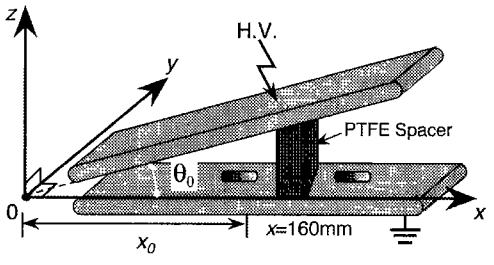

Fig. 1. Electrode and coordinate system

* Department of Electrical and Electronic Systems Engineering, ISEE, Kyushu University
6-10-1, Hakozaki, Higashi-ku, Fukuoka 812-8581
** Power Engineering R&D Centre, Tokyo Electric Power Co. (TEPCO)
Egasaki-cho, Tsurumi-ku, Yokohama 230-8510

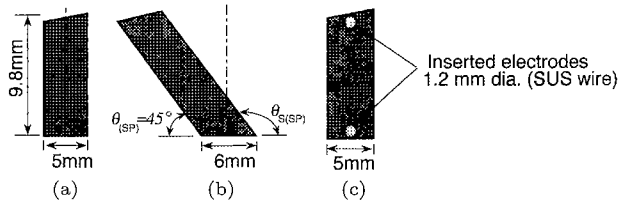

Fig. 2. Tested spacer(s) configurations: (a) T-SP, (b) C-SP, and (c) EI-SP

non-uniform field distribution along the electrode surface, a pair of non-parallel stainless-steel plates shown in Fig. 1 were used as an electrode system. The grounded electrode (G.E.) was arranged horizontally and the high voltage electrode (H.V.E.) inclined at an angle of 3.5° [7]. The Coulomb and the electrical gradient forces are almost at right angle with each other and the field strength is uniform along the electric lines of force but increases with decrease in the electrode gap length. When the coordinate system for this electrode arrangement is established as shown in Fig. 1 and it is assumed in the field calculations that fringing effect of the electrode is negligible, the field strength at point (r, θ) within the gap is given by equation (1), where V is the applied voltage and θ_0 (= 3.5°) is the angle between the plates. The electric lines of force in the diverging gap have only a θ component.

$$E_{r\theta} = V/r\theta_0 \cdots\cdots (1)$$

As shown in Fig. 2, different shaped spacers used in this study are; a) Trapezium spacer (T-SP) which simulates the disc-type spacer, b) shows slope spacers which simulates Cone-spacer (C-SP), and c) simulates the Electrode-Inserted spacer (EI-SP). Each tested spacer was mounted in the middle between the two electrodes, as shown in Fig. 1.

The applied voltage V is a positive or negative DC or 60 Hz AC voltage, generated by an arbitrary waveform generator (SG1200, Yokogawa) and is amplified by a factor of 2.0×10^3 by a HV amplifier (Model 20/20 A, Trek). In the measurement of particle motion onset voltages, the voltage was applied with ramped input of ~0.5 kV/s. On the other hand, in the observation of particle motion and the measurement of breakdown voltages, the voltage was applied with step input in order to make the observation easy and to simulate the practical voltage application.

In order to simulate the particles commonly found in GIS, each experiment was conducted using aluminum (Al.) wire particles of diameter $D(= 2a) = 0.25$ mm and length $L = 2 \sim 3$ mm whose ends were not rounded. The x-coordinate of the centre of the particle at the initial position on the G.E. shown in Fig. 1, is indicated by subscript 0, i.e., x_0.

Particle behavior was observed using CCD camera recording onto a video tape. Every experiment was conducted in laboratory air in order to make the experiment easy.

3. Wire Particle Motion Onset Voltages

When a charged conducting wire particle is within the test gap whose field distribution can be given by equation (1), the particle is mainly acted upon by; (i) the Coulomb force $F_q(= qE_0)$ in the direction of electric lines of force (in the θ direction), (ii) the gravitational force F_g in the $-z$ direction, (iii) the electrical gradient force F_{grad} in the direction of higher field regions (in the $-r$ direction), (iv) the viscous force F_v, (v) a repulsive force at the instant of particle collision with an electrode [8] and (vi) the effect of the reactive force due to electric wind [13] i.e. the effect of a resultant of the electrostatic force between the particle and the space charge, the force caused by the collision of electrons and ions at the wire particle's ends.

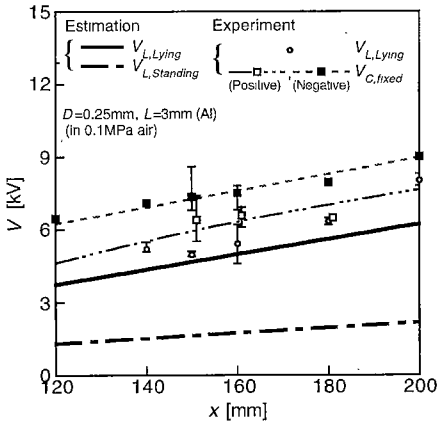

Fig. 3. Particle's lifting voltage and corona inception voltage as a function of x_0

With a wire particle of radius a (mm) and length L (mm), the charge (q) on a horizontally lying or vertically standing particle on an electrode, are given by equations (2) and (3), respectively [9]:

$$q_l = 2\pi\varepsilon_0 aLE_0, \cdots\cdots (2)$$
$$q_s = \pi\varepsilon_0 L^2 E_0/[\ln(2L/a) - 1] \cdots\cdots (3)$$

If the z-component of Coulomb force (F_{qz}) is larger than gravitational force (F_g) acting on a particle, it is known that the particle stands and lift up towards the H.V.E. Lifting electric field E_{lift} for particle's both positions i.e. lying and/or standing can be easily expressed as [9]:

$$(E_l)_{\text{lift}} = [\{a(\rho_p - \rho_s)g\}/(1.43\varepsilon_s\varepsilon_0)]^{1/2}, \cdots\cdots (4)$$
$$(E_s)_{\text{lift}} = [\ln(2L/a) - 1][\{a^2(\rho_p - \rho_s)g\}/ \{(\varepsilon_s\varepsilon_0 L\ln(L/a)) - 0.5\}]^{1/2} \cdots\cdots (5)$$

where ρ_p and ρ_s are the density of the particle and gaseous medium, respectively, ε_s and ε_0 are the relative permittivity of gaseous medium and vacuum, respectively and g is the gravitational acceleration.

In case of wire particle, an increase in the electric field above the lifting field will raise the particle from lying position to vertical position. Hence, initially the particle will be charged according to equation (2) and then immediately charged according to equation (3) as it is raised. Comparing equations (2) and (3) above, it can be seen that $q_s > q_l$, i.e. the particle vertically standing

in the gap acquires more charge and so become more active in the field. Therefore, as long as the wire particle is lifted from the horizontal position, it automatically acquires more charge, which makes it more influenced by the gap's field. As shown in Fig. 3, the solid and dotted line is the estimated lifting onset voltages for the lying or standing particle, calculated from equations (4) and (5), respectively. It is clearly evident from Fig. 3, that lifting onset voltage $V_{L(\mathrm{Lying})} > V_{L(\mathrm{Standing})}$. It is also clear from Fig. 3 that, the corona inception voltage for vertically standing particle is higher than the particle lifting voltage under the present condition.

4. Experimental Results and Discussion

4.1 Observation of Wire Particle Motion without Spacer

4.1.1 Without corona discharge Before explaining the motion of a corona-discharging wire particle, the particle motion without corona is discussed here. It was found that, under DC step voltage $V_L < V < V_{C,fixed}$, unlike a spherical particle [8], a wire particle lying on the G.E. immediately stands up, crosses the gap and collide with the upper H.V.E. Thereafter, the particle is reflected from the H.V.E. and oscillates between the two electrodes, advancing towards the increasing gap region by the effect of reflection angle upon impact with the H.V.E. There were also the cases when the wire particle was reflected in unexpected directions due to irregular shape of wire particle ends. In this case, no polarity effect of the applied voltage on particle motion behavior was observed.

Whereas, under 60 Hz AC voltage, the observed particle behavior without spacer is similar to that explained for DC voltage. The only difference is that, under low AC voltages, the particle initially bounce on the G.E. due to polarity reversal in every half cycle of the applied voltage and then lift toward H.V.E. when the lifting field is satisfied. Whereas, under DC voltage, the particle immediately lift up towards H.V.E. and then oscillate between the electrodes advancing towards the increasing gap region.

4.1.2 With corona discharge Since the characteristics of corona discharge changes with the polarity of the $V_{applied}$, the observation of wire particle motion under $V \geq V_{C,fixed}$ was conducted for positive or negative DC and 60 Hz AC voltages. The typical results are as shown in Fig. 4.

When positive DC voltage of $V = 10.5\,\mathrm{kV}$ was applied, a particle lying at $x_0 = 200\,\mathrm{mm}$ stood up on the G.E. with its top spinning as shown in Fig. 4(a), but did not lift although lifting field was satisfied. On the other hand, when negative DC voltage of $V = -10.5\,\mathrm{kV}$ was applied, the particle at $x_0 = 200\,\mathrm{mm}$ was lifted, crossed the gap and collided with the upper electrode. However, as shown in Fig. 4(b), the particle was not reflected from the electrode, but kept standing while spinning on the negative H.V.E. Whereas, under 60 Hz AC voltage, due to the polarity effect of the applied voltage, an unsteady spinning particle motion only on the G.E. was observed, as shown in Fig. 4(c). Although these tendencies correspond with the results of reference [11], there exists gradient in the electric field along the direction of the electrode surface in the present electrode system. Therefore, the particle which keeps standing while spinning on the negative electrode within a diverging gap can move laterally on the negative electrode by the action of forces acting in the direction along the electrode surface, causing the particle to trigger breakdown at high field positions, as shown in Fig. 4.

The polarity effect on the spinning particle behavior in the gap is clearly indicated from Figs. 4(a) and (b), which indicates that spinning wire particle always stand on the negatively charged electrode and can move easily in contact with the negative electrode. This is because, when $V \geq V_C$ is applied, the streamer corona discharge occurs at the positive end of the wire particle whereas Trichel corona is generated at the negative end of the particle [12]. In this case, negative Trichel corona occurs much more frequently than positive streamer corona. Therefore, the particle is acted upon by the reactive force due to electric wind of negative Trichel pulse corona which is stronger than that due to positive streamer corona [13], causing the particle to drift towards the negative electrode. So, when corona discharge is maintained at the wire particle tips, the particle tends to stand on the negative electrode and move laterally along the negative electrode surface.

4.2 Observation of Wire Particle Motion around Spacer

We know that in all GIS equipments, there is at least one insulating spacer subjected to rated voltage. The free conducting particle can easily reach the spacer surface, reducing the system withstand voltage. In an earlier paper [10], the authors reported the spherical particle motion behavior around different shaped spacer(s) in non-uniform field. However, the shape of the particle which is occasionally present in GIS are non-spherical, rather elongated or needle shaped. Although, wire particles exhibit almost

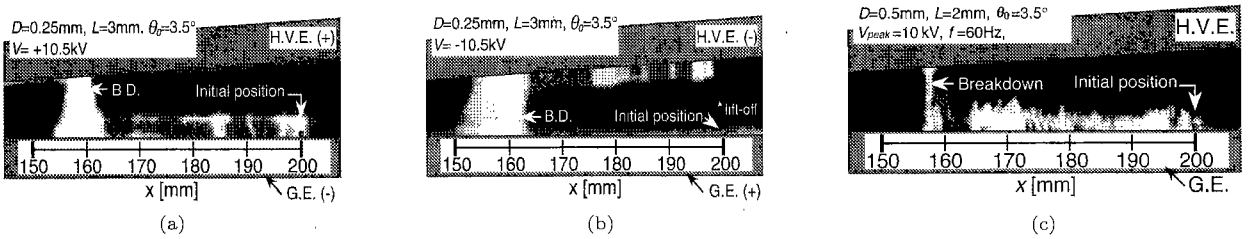

Fig. 4. Wire particle behavior with corona discharge under: (a) positive DC, (b) negative DC, and (c) 60 Hz AC voltage

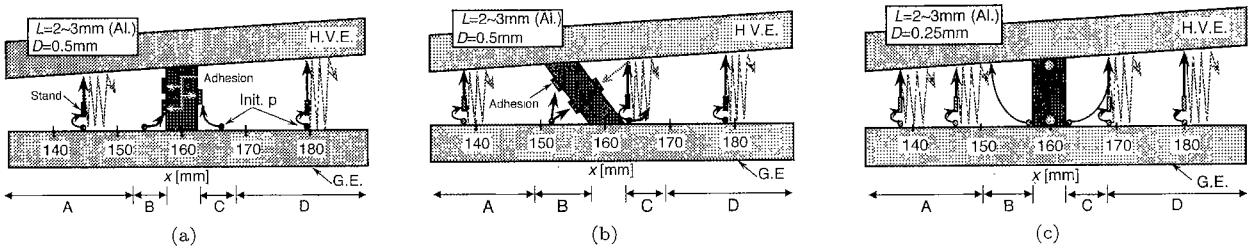

Fig. 5. Schematic diagram of wire particle behavior (withoud corona discharge) around spacer(s): (a) T-SP, (b) C-SP, and (c) EI-SP.

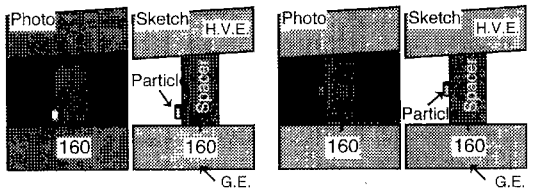

(a) Adhesion at the instant or particle levitation (b) Adhesion after oscillating motion

Fig. 6. Photoes and sketches of the particle adhered to T-SP

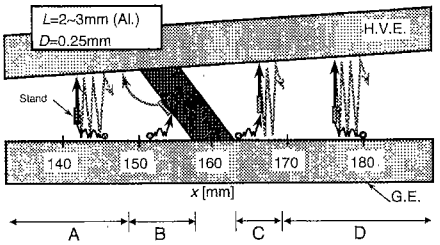

Fig. 7. Schematic diagram of wire particle motion around C-SP (under 60 Hz AC voltage)

similar basic behavior such as lifting, oscillation, etc., there were the cases where wire particles exhibit firefly [(1)(11)] or spinning motion. In order to investigate the free-conducting wire particle behavior in the presence of various shaped spacer(s) before breakdown, particle motion was observed (without and with corona discharge) around each tested spacer shown in Fig. 2 under DC and 60 Hz AC voltages while changing the particle initial position x_0.

4.2.1 Without corona discharge The schematic diagrams of the observed wire particle motion without corona discharge around various shaped spacers are as shown in Fig. 5. It was found that similar to spherical particle [(10)], the wire particle behavior around spacer can also be roughly divided into four types (A~D), depending on the particle initial motion behavior and also on the magnitude of the motion onset voltage. It can be seen that, when a wire particle is placed in Region A or D i.e. the region away from the spacer and the applied voltage $V_L < V < V_{C,fixed}$ is gradually increased, the particle would immediately lift, cross the gap and oscillate between the electrodes advancing towards increasing gap region. This observed free wire particle motion behavior around each spacer in Regions A and D was almost similar to particle behavior observed without spacer, as explained in Section 4.1.1 above. Whereas, the observed particle behavior (without corona discharge) in Regions B and C around each tested spacer, can be explained as follows:

(a) T-SP Under the DC applied voltage, the particle lying in Region B ($154 < x_0 < 157$ mm) or C ($163 < x_0 < 167$ mm) around T-SP, initially moved laterally toward the spacer at lower motion onset voltages as compared to without spacer and as soon as it reached the T-SP, the particle stood up and easily adhered to the spacer, as shown in Fig. 5(a). When the voltage was off, the particle remained adhered to the spacer surface. Whereas, under 60 Hz AC voltage, the particle oscillates around the spacer surface for longer time as compared to DC voltage and finally adhere to spacer. Moreover, the particle adhered to the spacer under AC voltage, rotates/rolls or slightly vibrates along the point of adhesion with the spacer surface. In this case, when the voltage is slightly increased further, the adhered particle can easily escape toward high field region, reducing the breakdown voltage.

Hence, under the DC applied voltage, the wire particle adhered to the spacer surface can hardly escape whereas under AC voltage it can easily escape toward high field region, reducing the withstand voltage. This kind of particle behavior under AC voltage is due to polarity change in every half cycle of the applied voltage. The photographs of the particle adhered to the spacer surface at the instant of particle levitation or adhesion of particle after oscillating motion between the electrodes under DC voltage is shown in Fig. 6.

(b) C-SP Under the DC voltage, the observed particle behavior in Region B ($150 < x_0 < 157$ mm) on the acute angle gap side of C-SP, as shown in Fig. 5(b), was similar to that as explained above in case of T-SP i.e. the particle tend to move toward C-SP. However, an interesting particle behavior was observed when the particle was placed on the obtuse angle gap side of C-SP in Region C ($163 < x_0 < 168$ mm). In this case, when the $V_{applied}$ is gradually increased, the particle in Region C initially moved laterally away from the spacer upto $x = 168$ mm and then lifts up and oscillates. Similar phenomenon in particle motion behavior was observed around C-SP under 60Hz AC voltage as well, as shown in Fig. 7. The particle adhered with spacer under AC voltage can easily escape toward high field region, when the voltage is slightly increased after the particle adhesion.

(c) EI-SP The wire particle in Regions B (152 <

$x_0 < 157\,\text{mm}$) and C ($163 < x_0 < 167\,\text{mm}$) around EI-SP initially moves away from the spacer as shown in Fig. 5(c) due to the electrostatic repulsive force between the free conducting particle and the inserted electrodes and then lifts and oscillates. The free oscillating particle around the EI-SP in Region B can finally adhere to the spacer. Moreover, it was also observed that under the same experimental conditions, the free particle around EI-SP oscillate for longer time than free particle oscillation time around T-SP, if the spacer surface charge is neglected.

The reason why the wire particle under DC voltage can firmly adheres to the spacer whereas under the 60 Hz AC voltage, the particle hardly adheres and can rotate/roll or vibrate along the point of adhesion, can be explained as follows. When a charged particle is in the vicinity of a spacer, despite various forces acting on the free conducting particle as explained in section 3, above, an additional force known as "image force or the induced electrostatic force" also acts on the particle in the direction perpendicular to the spacer surface. The image force (F_i) acting on a wire particle around a spacer is given by equation (6), below.

$$F_i = \left[\frac{\lambda^2}{4\pi\varepsilon_0 d^2}\right]\left[\frac{\varepsilon_2 - \varepsilon_1}{\varepsilon_2 + \varepsilon_1}\right] \times L^2 \quad \cdots\cdots\cdots\cdots \quad (6)$$

where, $\lambda = q/L$ i.e. charge per unit length on the wire particle and d (mm) is the distance of particle from the spacer.

If we numerically calculate the various forces acting on the particle i.e. $F_q(= qE_{r\theta})$, $F_g(= \pi {r_p}^2 Lg(\rho_p - \rho_0))$, F_i, etc., the results can be seen from Fig. 8. Which indicates that in the vicinity of the spacer, the only effective force on the particle is F_i due to which the particle remains adhered to the spacer surface.

Whereas, under the AC voltage, the electrostatic force acting on the adhered particle changes its direction as well as its magnitude in every half cycle of the applied voltage, due to which the particle can easily rotate/roll or vibrate along the spacer surface. During this time, if the electrostatic force between the adhered particle and nearest electrode overcomes the force of attraction between the particle and spacer, the particle can easily escape toward high field region and triggers breakdown.

Particle motion (without corona discharge) observed around different shaped space(s) was different depending on the spacer configuration. For example, when the field strength around the spacer was higher than the external

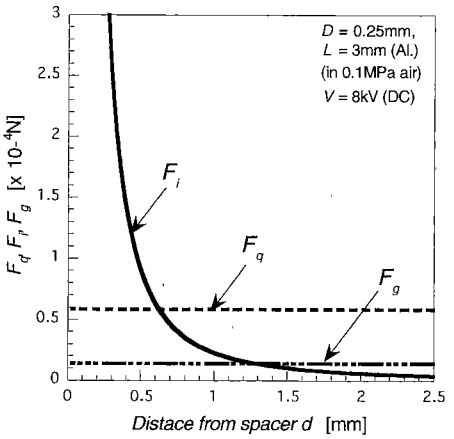

Fig. 8. Simulation results of image force acting on particle around T-SP

gap field strength, the particle tends to move towards the spacer, as explained above in case of T-SP or the acute angle gap side of C-SP. On the other hand, in case of lower field strength in the vicinity of the spacer than the external gap field such as on the obtuse angle gap of C-SP or around EI-SP, the particle tends to move away from the spacer towards the higher field region under both DC and/or 60 Hz AC voltages.

4.2.2 With corona discharge When one of the spacers under consideration i.e. T-SP, C-SP, or EI-SP was mounted between the two electrodes at $x = 160\,\text{mm}$ and wire particle motion was observed around these spacers under $V \geq V_C$. The observed particle behavior (with corona discharge) under the positive or negative DC or 60 Hz AC voltage, is as explained below:

(a) Under positive DC The schematic diagram of the wire particle motion with corona discharge around the tested spacers under the positive DC step voltage ($V \geq V_C$) is as shown in Fig. 9. It was found that upon the application of positive DC step voltage, particle in Region A on the G.E. behaved similar to the behavior of corona discharging particle without spacer as explained in section 4.1.2, above. However, the particle lying near T-SP in Regions B and C, as shown in Fig. 9(a), the particle started spinning and moved laterally towards the spacer in $+x$ and $-x$ directions, respectively at lower motion onset voltages. When this spinning particle reached the spacer, it may not adhere to the spacer surface but reversed its direction of motion at about $x = 156\,\text{mm}$ and 165 mm and moved laterally away from the spacer while spinning.

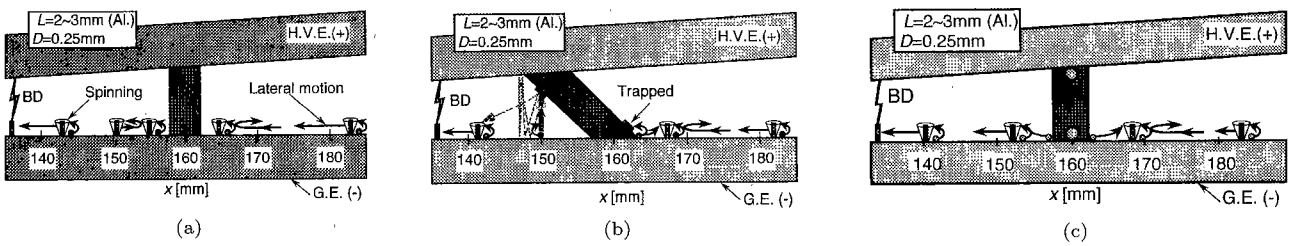

Fig. 9. Schematic diagram of wire particle behavior with corona discharge around spacer(s) (Under Positive DC voltage): (a) T-SP, (b) C-SP, and (c) EI-SP

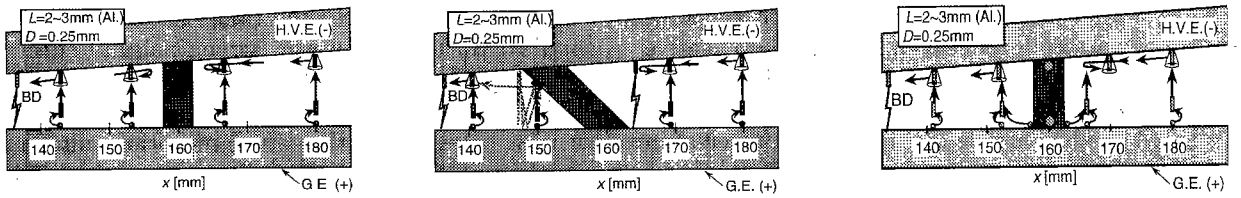

Fig. 10. Schematic diagram of wire particle behavior with corona discharge around spacer(s) (Under Negative DC voltage): (a) T-SP, (b) C-SP, and (c) EI-SP

Similarly, when a particle was present very close to C-SP on the acute angle gap side, as shown in Fig. 9(b), the particle started spinning motion on the G.E. after being reflected from spacer and moved laterally towards decreasing electrode gap region while spinning. On the other hand, on the obtuse angle gap side of the C-SP, the particle laterally moved away from the C-SP upto $x = 168$ mm and then started spinning motion.

Also, in Regions B and C around EI-SP as shown in Fig. 9(c), the particle was repelled away from the spacer due to electrostatic repulsive force between the particle and inserted electrodes. The particle stood up at about $x = 152$ mm and $x = 167$ mm, respectively, with its top spinning and moved laterally away from the EI-SP on the negative G.E.

(b) Under negative DC Schematic diagram of wire particle motion with corona discharge around tested spacers under negative DC ($V \geq V_C$), is as shown in Fig. 10.

A wire particle around T-SP in Regions B and C, immediately crossed the gap and moved toward T-SP while spinning along the H.V.E. as shown in Fig. 10(a). The particle in spinning motion did not adhere to spacer surface in this case as well but, reversed its direction of motion at about $x = 155$ mm and 165 mm.

Similarly, a particle in Region B around C-SP was lifted up, got reflected toward negative electrode after collision with spacer and started spinning motion as shown in Fig. 10(b). Whereas, on the obtuse angle gap side, a particle while spinning moved along the H.V.E. towards obtuse angle gap of spacer and returned back. Sometimes breakdown also occurred when the particle tended to enter this region.

In case of EI-SP as shown in Fig. 10(c), a particle lying in Regions B and C, was repelled away from the spacer, lifted up towards the H.V.E. and was not reflected from the upper electrode, moved along the upper negative electrode surface towards the high field regions while spinning. When the particle approached near the EI-SP in Region-C, it was reflected back and reversed its direction of advance in the direction away from the EI-SP at about $x = 167$ mm, due to the electrostatic repulsive force and repeat this motion behavior.

(c) Under 60 Hz AC voltage When the particle is in Region A or D, similar unsteady corona discharging particle behavior on the G.E. only was observed under the AC voltage, as explained in section 4.1.2, above. Whereas, when the particle was in Region-B or C around T-SP or in Region B on the acute angle gap of C-SP,

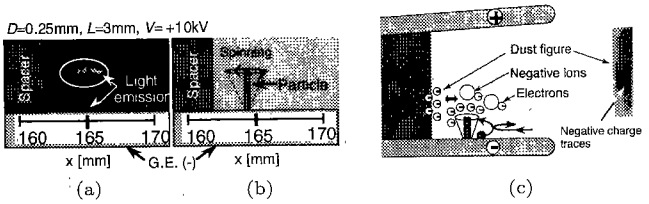

Fig. 11. Result of observation of corona discharge: (a) Light emmision from corona, (b) spinning particle position, and (c) dust figure results

as shown in Fig. 9, it was observed that when the field strength in the vicinity of spacer is stronger than the external field strength, the particle tends to move towards spacer while spinning. On the other hand, on the obtuse angle gap side of C-SP or around EI-SP, the spinning particle tend to move away from the spacer. Sometimes, this unsteady spinning particle may adhere to the spacer surface but can easily get free toward high field region, as explained in section 4.2.1 above.

Therefore, it can be concluded that, the obtuse angle gap of C-SP and EI-SP can not only reduce the field strength around the triple-junction but also suppresses both the particle motion toward spacer and particle's adhesion to the spacer.

As described above, the wire particle without corona discharge around spacer can easily adhere to the spacer. When the voltage was off, the particle remained adhered with the spacer surface and did not fell down. While a spinning particle under DC voltage as shown in Fig. 9 and 10, may not be adhered to spacer surface but reverses its direction of advance due to the repulsive force between the charges on the spinning wire particle and the space charges adhering to spacer surface produced by the steady corona discharge at wire particle ends, as shown in Fig. 11.

In order to confirm this consideration, dust figure technique was used. The dust used in this method was ordinary copier toner of negative polarity. Representative results of dust figures for the T-SP under the positive step voltage applications ($V \geq V_C$) are shown in Fig. 11(c).

Negative charge traces were observed when a particle exhibited spinning motion around the spacer, as shown in Fig. 11(c). These results can easily explain why a spinning particle does not adhere to the spacer and reverses its direction of advance.

The reason why the unsteady spinning particle under the AC voltage can easily adhere to the spacer, can be easily explained as follows. When an unsteady corona

discharging particle reach an insulating spacer, the force of electrostatic attraction between the induced negative charges on the spacer surface due to the spinning wire particle around spacer as shown in Fig. 11, and the opposite charge on the particle due to polarity reversal in every half cycle, the particle can easily adhere to the spacer.

5. Breakdown Characteristics

In order to make the experiment easy and to make the free conducting particle to easily oscillate along the PTFE cylindrical shaped spacer (Spacer height = 10 mm), a concave-cone shaped H.V.E. was used. This H.V.E. was designed such that the angle between the edge and the center of the circular H.V.E. was 3.5° to the horizontal plane G.E. Aluminium wire particles of diameter $D(=2a) = 0.25$ mm and length $L = 3$ mm were used as test particles. Distance between the conducting particle's centre and G.E. along the spacer surface is denoted by h [mm]. Surface flashover voltages were measured under ramped DC or AC voltages increased at a rate of 0.5 kV/s for a particle artificially fixed to the spacer and for a particle which was initially free but finally adhered to the spacer after levitation as explained in Section 4.2, above.

The wire particle triggered breakdown voltage characteristics both under DC and AC voltages for free oscillating particle, the initially free (but adhered to spacer after levitation) and artificially fixed particle are as shown in Fig. 12. It is clearly indicated in Fig. 12 that $V_{L(\text{standing})}$ (≈ 1.8 kV) is less than that $V_{L(\text{Lying particle})}$ (≈ 4.9 kV), as the particle vertically standing in the gap acquires more charge as compared to lying particle and become more active in the field as explained in section 3, above. After lifting, the particle will either oscillate and triggers breakdown (5.4~7.5 kV) or adheres to spacer surface due to increased electrostatic force (image force) between the particle and spacer. When V_{BD} for the initially free (but adhered to spacer after levitation) particle are compared to those for artificially fixed particle, V_{BD} for both the

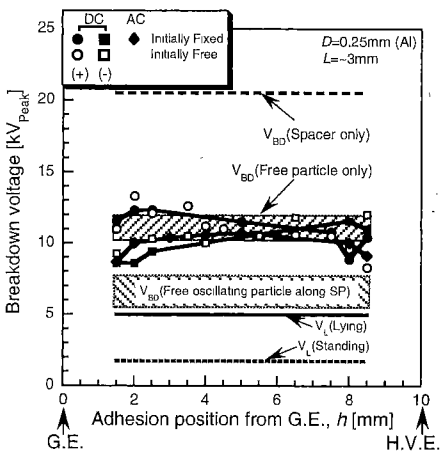

Fig. 12. Breakdown characteristics for initially free and fixed wire paritcle around cylindrical spacer

cases were almost in same range for both DC and AC applied voltages. However, strong polarity effect in the breakdown voltage characteristics were observed under the DC voltage, as shown in Fig. 12. On the other hand, it was observed that the corona inception voltage for the adhered particle for both the positive and negative DC applied voltages, disperse widely around the $V_{C(Fixed)}$. This may be because the field strength at the tip of the particle, that depends on the magnitude and polarity of the charge on the particle. That is, the field strength at the tip of an adhered particle is stronger than the artificially fixed particle. So the V_C (minimum) for free particle will be lower than artificially fixed particle. However, when a charged particle adheres to a spacer, partial discharge may occur between the particle and the spacer. In this case, the charge on the particle tips is reduced and at the same time the field distribution will also be changed by the presence of the surface charges produced by the PD. In this case, the subsequent corona can hardly occur until the applied voltage is significantly increased. Since V_C is measured after the particle adhesion with the spacer in this study, the above mechanism might affect the relation between V_C's for free and artificially fixed particles. Almost similar corona and breakdown voltage characteristics were also observed for the other shapes of the tested spacers.

6. Concluding Remarks

In this work, the wire particle motion behavior and particle initiated breakdown characteristics around different shaped spacers between diverging conducting plane electrodes were investigated under DC and 60 Hz AC voltages in atmospheric air. The obtained results can be summarized as follows

(1) Free conducting particle around different shaped spacers tends to move towards or away from the spacer depending on the field strength at the triple junction.

(2) Conducting particle can be prevented from approaching the spacers, by using the: (i) Obtuse angle gap of spacer, and (ii) Inserting electrodes in the spacer.

(3) Free conducting wire particle without steady corona discharge under DC voltage can easily adhere to the spacer and hardly escape toward high field region. Whereas under the AC voltage, the particle adhered to spacer rotate/roll/vibrate along the point of adhesion and can easily get free.

(4) Free conducting wire particle with steady state corona discharge under the DC voltage can hardly adheres to the spacer, whereas, under the non-steady state corona discharge under the AC voltage, the particle sometime may adhere to the spacer surface but can easily escape.

(5) Breakdown voltage for artificially fixed particle is almost equal to that for adhered particle under both DC and AC voltages. However, under the AC voltage, the particle adhered to the spacer can easily escape toward high field region reducing the withstand voltage.

Hence, the insulation condition in GIS equipment under the AC voltage become more severe.

The present work is a basic research, therefore to make

the experiment easy, the particle behavior around different shaped spacers was studied in the laboratory air only. Similar phenomena will also appear in the SF_6 gas as well, if no partial discharges such as corona discharge or microdischarge occur. But if electrical discharges occur [14], the effect of gas on the particle motion around the spacer should be confirmed, as the characteristics of corona discharge depends on gas.

(Manuscript received Feb. 20, 2003,
revised June 2, 2003)

References

(1) C.M. Cooke, R.E. Wootton, and A.H. Cookson: "Influence of Particles on AC and DC Electrical Performance of Gas Insulated Systems at EHV", *IEEE Trans. PAS*, Vol.96, No.3, pp.768–777 (1977)

(2) A. Diessner and J.G. Trump: "Free Conducting Particles in a Coaxial Compressed Gas Insulted System", *IEEE Trans. PAS*, Vol.89, No.8, pp.1970–1978 (1970)

(3) A.H. Cookson, O. Farish, and G.M.L. Sommerman: "Effect of Conducting Particles on AC Corona and Breakdown in Compressed SF_6", *IEEE Trans. PAS*, Vol.91, pp.1329–1338 (1972)

(4) M. Hara and M. Akazaki: "A method of Prediction of Gaseous Discharge Threshold Voltage in the Presence of a Conducting Particle", *J. Electrostatics*, Vol.2, pp.223–239 (1976/1977)

(5) F.A.M. Rizk, C. Masetti, and R.P. Comsa: "Particle Initiated Breakdown in SF_6 Insulated Systems under High Direct Voltages", *IEEE Trans. PAS*, Vol.98, No.3, pp.825–836 (1979)

(6) J.R. Laghari and A.H. Qureshi: "A Review of Particle Contaminated Gas Breakdown", *IEEE Trans. EI*, Vol.16, No.5, pp.373–387 (1981)

(7) T. Hasegawa, K. Yamaji, M. Hatano, F. Endo, T. Rokunohe, and T. Yamagiwa: "Development of Insulation Structure and Enhancement of Insulation Reliability of 500 kV DC GIS", *IEEE Trans. PWRD*, Vol.12, No.1, pp.194–202 (1997)

(8) K. Sakai, D.L. Abella, S. Tsuru, and M. Hara: "Conducting Particle Motion and Particle initiated Breakdown in dc Electric Field between Diverging Conducting Plates in Atmospheric Air", *IEEE Trans. DEI*, Vol.6, No.1, pp.122–130 (1999)

(9) R.E. Wooten, A.H. Cookson, F.T. Emery, and O. Farish: "Investigation of HV Particle Initiated Breakdown in Gas Insulated Systems", EPRI EL-1007 (1979)

(10) Y. Khan, K. Sakai, E-K. Lee, J. Suehiro, and M. Hara: "Free Conducting Spherical Particle Motion Behavior around Different Shaped Spacers under DC Voltage", Proc. of 12th ISH, Vol.2, pp.294–297, Bangalore (2001)

(11) Y. Higashiyama: "Influence of DC Corona Discharge on the Behavior of a Filamentary Particle between Parallel Plane Electrodes", Proc. of 11th International Conf. on Gas Discharge and their Applications, Vol.1, pp.188–191 (1995)

(12) M. Akazaki and M. Hara: "Mechanics and Characteristics of DC Corona from Floating Particle", *J. IEE Japan*, Vol.90, No.4, pp.131–141 (1970)

(13) K. Sakai, D.L. Abella, J. Suehiro, and M. Hara: "Lateral Motion of Wire Particles toward Decreasing Electrodes Gap Regions in Atmospheric Air", Proc. of 6th ICPADM, Vol.2, pp.817–820, Xi'an (2000)

(14) K. Sakai, D.L. Abella, Y. Khan, J. Suehiro, and M. Hara: "Experimental Studies of Free Conducting Wire Particle Behavior between Non-Parallel Plane Electrodes with ac Voltages in Air", *IEEE Trans. DEI*, Vol.10, No.3, pp.418–424 (2003)

Yasin Khan (Student Member) was born in Peshawar, Pakistan on February 2nd, 1971. He received the B.Sc. and M.Sc. degrees in Electrical Engineering from the N.W.F.P. University of Engineering and Technology, Peshawar in 1993 and 1997, respectively.From 1995 to 2000, he was working in the Energy Wing, Planning Commission, Govt. of Pakistan, Islamabad as a Research Officer (Power). Since 2000, he is a Doctor course student in Kyushu University, Fukuoka, Japan. Mr. Khan is member of the Pakistan Engineering Council (PEC) and an associate member of the Institute of Electrical Engineers, Japan (IEEJ).

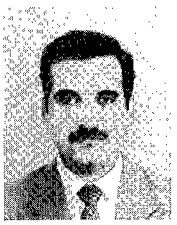

Akihito Oda (Student Member) was born in Fukuoka Prefecture, Japan on June 14th, 1978. He received the B.Sc. degree in Electrical Engineering from the Kyushu University, Fukuoka, Japan in 2001. Currently, he is Master Course student in Kyushu University, Japan. Mr. Oda is an associate member of the Institute of Electrical Engineers, Japan (IEEJ).

Shigemitsu Okabe (Member) was born on September 9th, 1958. He received the Dr.Eng. degree in Electrical Engineering from Tokyo University, Japan in 1986. From April, 1986 he joined Tokyo Electric Power Co. (TEPCo.). Mr. Okabe was a visiting researcher in the Munich Engineering University, Munich, Germany in 1992. Now, he is Group Manager of the Power Engineering R&D Center at TEPCo. He is a member of IEEE.

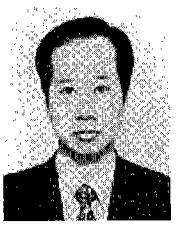

Junya Suehiro (Member) was born in Fukuoka Prefecture, Japan on March 9, 1961. He received M.S. and Dr.Eng. degrees in electrical engineering from Kyushu University in 1985 and 1991 respectively. He was with the Nippon Steel Co. from 1985 to 1988. Since April 1988, he has been at Kyushu University. He is now an Associate Professor and is involved in research on applied electrostatics and high voltage engineering at Kyushu University. Dr. Suehiro is a member of the Institute of Electrical Engineers of Japan, the Institute of Electrostatics Japan, the Cryogenic Association of Japan and the Institute of Engineers on Electrical Discharges in Japan.

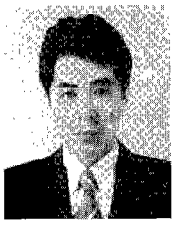

Masanori Hara (Member) was born in Kagawa Prefecture, Japan, on April 13, 1942. He received the M.S. degree and the Dr.Eng. degree from Kyushu University, Fukuoka, Japan, in 1969 and 1972 respectively. He served at Kyushu Institute of Technology as a Lecturer from 1972 to 1973 and as an Associate Professor from 1973 to 1975. In 1975, he moved to Kyushu University as an Associate Professor of the Department of Electrical Engineering. Since 1986, he is a Professor of the Department of Electrical and Electronic Systems Engineering, in the same university. Dr. Hara is a member of the Institute of Electrical Engineers, Japan (IEEJ), the Institute of Electrostatics, Japan, the Cryogenic Society of Japan and the Institute of Engineers on Electrical Discharges in Japan (IEEDJ). Now, he is a Vice-President of IEEJ and a President of the IEEDJ.